

PHOTOCATALYTIC DEGRADATION OF METHYLENE BLUE IN PRESENCE OF ZnO NANOPOWDERS SYNTHESIZED THROUGH A GREEN SYNTHESIS METHOD

T. K. MANDAL^{1*}, S. P. K. MALHOTRA¹, R. K. SINGHA²

¹IcfaiTech School, ICFAI University Dehradun, Rajawala Road, Selaqui Dehradun-248197, India

²Nanocatalysis Division, Indian Institute of Petroleum, Dehradun – 248005, India

Photocatalytic degradation of methylene blue was studied using ZnO nanopowders prepared through a green synthesis process. An aqueous solution of methylene blue was investigated in an open vessel equipped with sun light using ZnO nanopowders, as catalyst, with a concentration of 7.815×10^{-6} M. ZnO nanomaterials, prepared through a green synthesis method, was characterized with XRD, FTIR, SEM, EDX and BET measurements. The photodegradation of methylene blue in terms of concentration change with respect to different time intervals was studied with the UV-vis spectroscopy. The mechanism for this photocatalytic degradation process has also been presumed.

Keywords: ZnO nanopowders, Green synthesis, XRD study, FTIR study, Photocatalytic degradation, UV-vis study

1. Introduction

Environmental pollution has drawn much attention to the vital need for developing new ecofriendly purification technologies [1-7]. Toxic effluents from industries are a matter of serious concern for the environment, and much attention has been drawn toward the removal of harmful contaminants from waste water. Photodegradation of organic pollutants in aqueous solution is a promising method for environmental purification [1]. Extensive researches have been carried out for the search of materials in effective photodegradation ability. Recently, ZnO nanomaterials have been observed to have important application in improved photocatalytic degradation of dyes. Many researchers have reported their achievements in preparing ZnO nanomaterials and its composites through different methods and their improved application in photocatalytic degradation of organic dyes.

Liu et al have synthesized the nanocomposite of ZnO with CuO, applying low-temperature hydrothermal and photodeposition processes, for the environmental purification purposes [2]. Nabid et al reported the preparation ZnO/Fe₃O₄/PANI nanocomposites in order to enhance the photocatalytic efficiency of ZnO nanoparticles under visible light [3]. ZnO/ZnAl₂O₄ composite hollow

microspheres have been fabricated using glucose as template by a polyethylene glycol assisted one-pot hydrothermal method and the photocatalytic activity of the as-prepared samples was evaluated by photocatalytic decolorization of methyl orange [4]. Well-aligned ZnO nanorods were grown on indium–tin-oxide slide by the hydrothermal method and used as templates for preparing ZnO/Au composite nanoarrays by Sun et al. The composite was reported by them to have improvement of photocatalytic efficiency [5]. Recently, Bai et al prepared ZnO_{1-x}/graphene hybrid photocatalyst via a facile in-situ reduction of graphene oxide and ZnO_{1-x} surface defect oxide for the photodegradation of methylene blue [6]. Zhang et al prepared the ZnO/carbon quantum dots heterostructure via a sol–gel approach combined with a spin-coating processing for the enhancement of photocatalytic property [7]. Hu et al prepared ZnO nanoparticles by one pot fabricated direct precipitation and they used the as prepared sample for decoloring methyl orange under sunlight [8]. Khayyat et al reported Cd-doped ZnO multipods, synthesized by facile hydrothermal process and the multipods were used for environmental remediation applications. Photocatalytic degradation of acridine orange was investigated by them. They demonstrated that doped ZnO materials could be used as efficient photocatalyst for the photocata -

* Autor corespondent/Corresponding author,
E-mail: dr.mandal@iudehradun.edu.in

lytic degradation of various organic dyes and chemicals [9]. Xu et al reported that graphene hybridized with ZnO could produce an efficient photocatalyst [10]. A facile method is introduced to prepare large-area gold-coated ZnO nanorods, featuring the capability to tailor both the spatial distribution and the concentration of metal nanocrystals by Wang et al [11]. Liu et al reported the fabrication of a highly flexible, sensitive, and excellent reproducible photo-detector based on flexible nanoparticle-assembled ZnO cloth, which was synthesized via a carbon cloth templated hydrothermal method [12]. Well-crystalline flower-shaped ZnO nanostructures were synthesized by simple hydrothermal process at low-temperature of 145 °C and utilized as a photocatalyst and photo-anode material for photocatalytic degradation of Rhodamine B and dye-sensitized solar cell applications, respectively by Umar et al [13]. Satish Kumar et al prepared the Ag doped ZnO nanocomposites by simple material synthesis route and the as prepared material was potentially utilized for the photocatalytic degradation of an azo dye in the visible region [14]. An attempt has been made for the photocatalytic degradation of polyvinyl chloride using ZnO as semi-conductor catalyst in the form of PVC–ZnO composite film by Chakrabarti et al [15]. The photocatalytic decomposition of eco-persistent toluene, salicylic acid and 4-chlorophenol with sun light in an oxygenated aqueous suspension has been studied by Shinde et al under nanocrystalline hexagonal ZnO photocatalyst [16]. The ZnO-mediated photocatalysis process has been successfully applied to degradation of commercial dye, CI Reactive Blue 160 (RB 160) by Bansal et al [17]. In their work, eleven reaction intermediates were separated, identified and characterized by the GC–MS techniques, giving insight into mechanistic details of the ZnO-mediated catalysis process under UV irradiation and the pathways of degradation process. Their work explained how dopant modifies the characteristics of ZnO which helps in degradation of dyes in colored wastewaters [18]. Magnesium doped ZnO nanoparticles were synthesized through an oxalate coprecipitation method by Etacheri et al and they found superior sunlight-induced photocatalytic decomposition of methylene blue (MeB) in contrast to undoped ZnO [19]. It has been demonstrated by Taccola et al that zinc oxide nanoparticles induce death of cancerous cells whilst having no cytotoxic effect on normal cells [20]. Thurber et al reported a new method to improve a recent demonstration of ZnO nanoparticles selectively killing certain human cancer cells, achieved by incorporating Fe ions into the ZnO nanoparticles [21].

Recently, an attempt has been made to prepare reduced graphene-oxide/Titanium dioxide/Zinc oxide (rGO/TiO₂/ZnO) ternary

photocatalyst system via a facile two step solvothermal method and their results were compared with rGO/TiO₂ and TiO₂. The photocatalytic degradation of the system was investigated using a model dye MeB. The degradation efficiency of rGO/TiO₂/ZnO, rGO/TiO₂ and TiO₂ was found to be 92%, 68% and 47% within 120 min respectively. Their results pave the way for the development of futuristic rGO based ternary nanocomposites for photocatalytic applications [22]. A novel Ag/ZnO/C plasmonic photocatalyst was synthesized *via* a facile calcination and photodeposition route [23]. It showed from this study that Ag and ZnO nanoparticles sized 5–10 nm were uniformly dispersed on the surface of the carbonaceous layers in Ag/ZnO/C composites. The results indicated that the obtained Ag/ZnO/C sample exhibited higher adsorption capacity and enhanced UV and visible light driven photocatalytic activity to TC-HCl in compare to ZnO/C and pure ZnO. This research shows a simple and new route for the design of ZnO-based catalysts that respond to both UV and visible light and promotes their practical application in different environmental and energy issues associated with solar light. A facile route for the synthesis of ZnO–C nanocomposites using zinc citrate dihydrate as a precursor through one-step calcination under a nitrogen atmosphere has been reported by Xue et al [24]. The as-prepared ZnO–C nanocomposites, with 5–10 nm in size, exhibited enhanced photocatalytic activity compared to pure ZnO with respect to MeB degradation under UV irradiation, which was ascribed to the better separation of photogenerated electrons and holes in the presence of carbonaceous layers. In particular, the rate of degradation of MeB with ZnO as a photocatalyst was 4.15 times faster than that of using bare ZnO nanoparticles. Wang and coworkers reported a simple and green method for preparing the ternary photocatalyst Ag-graphene quantum dots ZnO [25]. The photocatalytic tests involving the degradation of Rhodamine B showed that the synthesized ternary photocatalyst displayed excellent visible-light photocatalytic activity, which was much higher than those of pure ZnO and binary photocatalysts such as Ag-ZnO and GQDs-ZnO. ZnO was prepared using microemulsion method [26]. In presence of visible light C doped ZnO obtained by calcining precursor at 300 °C shows better photocatalytic activity for MG degradation.

Thus, several methods have been reported for the synthesis of ZnO and its nanocomposites for the application in photocatalytic degradation of organic dyes. Search for a cheap, easy and ecofriendly method for the preparation of ZnO for the use of photocatalytic degradation process, is of importance. The present paper addresses an eco-friendly novel and new green synthesis method for

the preparation of ZnO nanopowders, which can effectively act as a better photodegradation material. The as prepared ZnO nanopowders have also been explored for the photodegradation of MeB, a representative dye. The concentration change of MeB in terms of absorbance change has been measured with UV-vis spectroscopy. A probable mechanism for the photocatalytic degradation of MeB in presence of ZnO nanopowder has also been presumed.

2. Materials and methods

The synthesis of ZnO nanomaterials have been carried out using green synthesis method which is a modified method [27, 28] as reported earlier, in which Zn^{2+} metal ions are dispersed in a aloe vera matrix gel, dried at around 70°C and the precursor mass was calcined at 500 °C for 2h. It formed in a stable transparent solution with Zn^{2+} metal cations rearranged in a specific structure through the aloe vera molecules. An amorphous structure of the precursor solution was retained after drying it at room temperature or even at higher temperatures in the 70 to 80°C ranges. The product was pulverized by grinding in a mortar with a pestle by hand. This carbonaceous mass was decomposed at 500°C in air, leaving behind a recrystallized ZnO nanopowder. X-ray diffraction of the specimen was recorded with PW 1710 X-ray diffractometer using 0.15418 nm $CuK\alpha$ radiation. Average crystallite size D was calculated from widths $\Delta 2\theta_{1/2}$ in the characteristic peaks with the Debye-Scherrer formula. The surface morphology of the as prepared nanocomposites was studied with a SEM of JEOL JSM-5800 (Tokyo, Japan) with an accelerated voltage of 20 kV. The specific surface area was measured by the single point BET method with liquid N_2 (Flowsorb 2300, Micromeritics Instrument Corp., Norcross, GA).

Methylene blue was purchased from Sigma Chemia GMBH (Germany) and used without further purification. The photocatalyst used in this work was the as prepared ZnO with surface area 45 m^2/g . The reaction mixture was carried out using 100 ml Pyrex glass reservoir placed outside the laboratory building. Pyrex glass beaker containing MeB sample (50 ml) and 20 mg of the ZnO catalyst was placed in the reaction vessel. The concentration of MeB was 7.815×10^{-6} M. Sunlight was collected by using concave lens with a focal length of 250 mm. The solution was kept homogeneous by using a magnetic stirrer in the suspended colored solution dye. The time of irradiation was in between 10.00 AM to 3.00 PM. The UV-Vis spectrum of MeB, photocatalysed with ZnO nanopowder, was measured using spectrophotometer (Perkin Elmer, Lambda 25). The UV-Vis spectrum measurement was calibrated and standardized with proper wavelength selection.

3. Results and discussion

The phase formation of the as prepared ZnO nanopowders has been studied with the help of XRD analysis. Figure 1 shows the XRD of ZnO nanopowders processed by heating the aloe-vera precursor in air at 500°C for 2h.

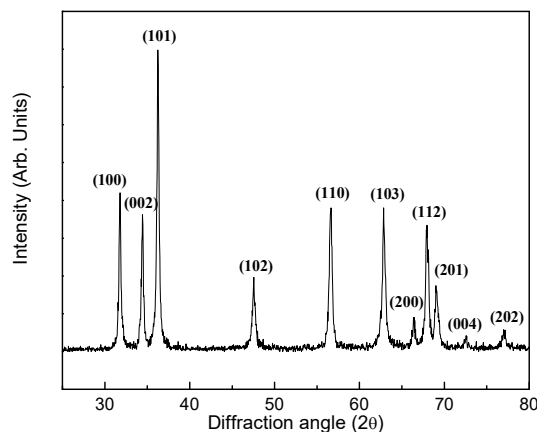


Fig. 1 - The X-ray diffractogram of ZnO nanopowders prepared by heating the aloe-vera based ZnO precursor material at 500 °C for 2h.

XRD of ZnO indicates the well-defined hexagonal shape with the $P6_3mc$ space group, resulted by calcining the aloe-vera based ZnO precursor at 500°C for 2h. The peaks observed in the diffractogram in Figure 1 are assigned in terms of the Miller indices (hkl) assuming a hexagonal crystal structure of ZnO, with the lattice parameters $a = b = 0.3253$ nm and $c = 0.5209$ nm [16]. The most intense peak (relative intensity $I = 100\%$) in the diffractogram lies at 0.2478 nm in (101) reflection. The second and third most intense peaks lie in (100) and (002) reflections at 0.2815 nm and 0.2597 nm, respectively (Table 1). Thus, various well-defined dominant diffraction reflections are seen in the observed XRD pattern which are all related and well matched with the diffraction reflections of hexagonal phase ZnO. Average crystallite size as measured from XRD using the Debye-Scherrer formula is 30 nm [17-19]. These D values refer to average values calculated by $\Delta 2\theta_{1/2}$ in the (101), (100), (110), (002) and (112) etc prominent peaks of the diffractogram. The D values were also calculated applying Williamson-Hall integral breadth method [20]. In this method the selected peaks were fitted in a computer program (X'Pert HighScore Plus). With this program the value of $\sin\theta$ and β (FWHM, which is defined as $\int I(2\theta)d(2\theta) / I_{max}$) were calculated for each peak. D values were obtained from the intercept of the plot of β vs. $\sin\theta$ of the prominent peaks, using the relation $\beta = 1/D + 4e.\sin\theta/\lambda$ [where: β ((degrees) = FWHM; dimensionless, D (nm) = crystallite size; dimension

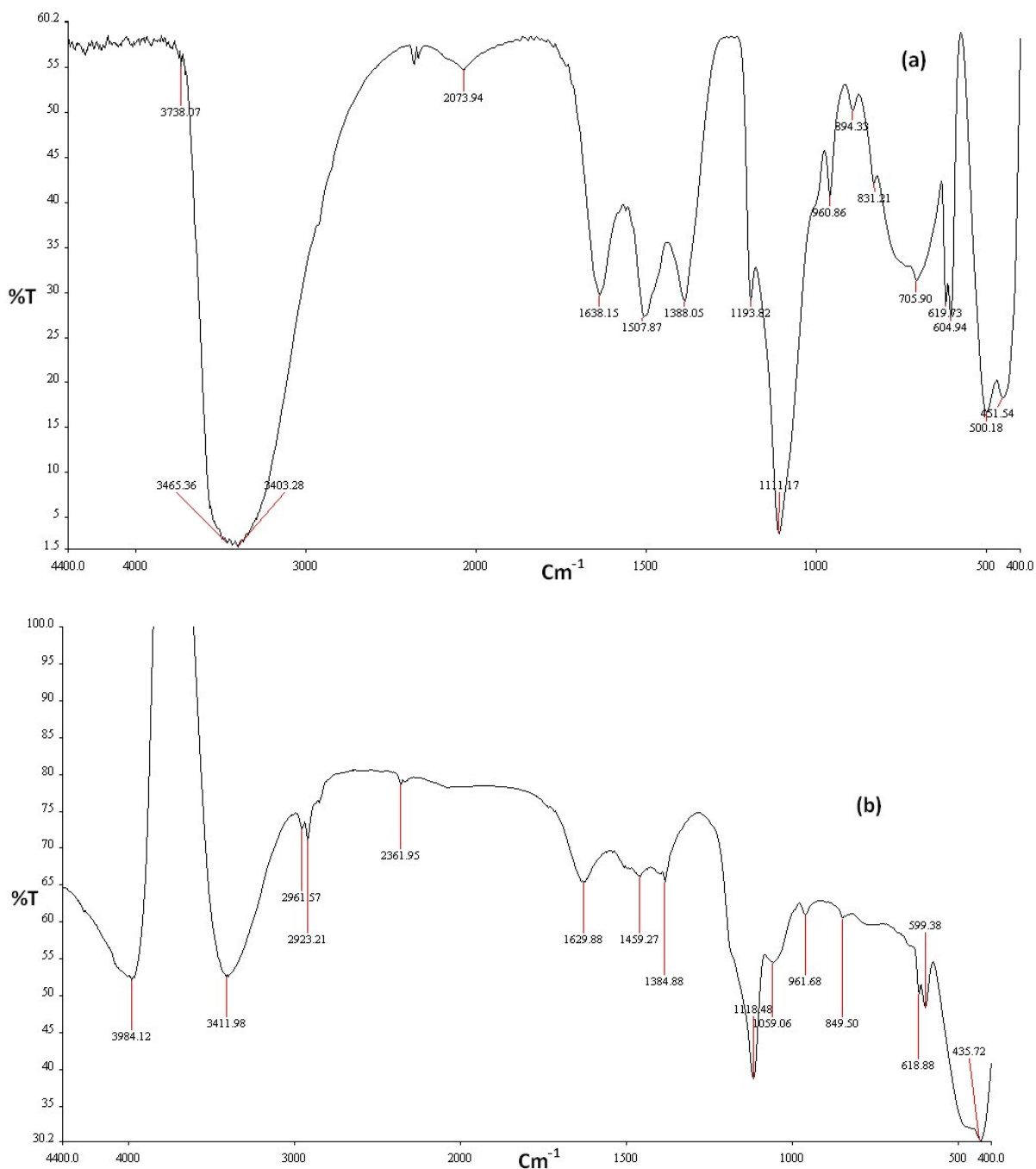


Fig. 2 - The FTIR spectra of (a) aloe-vera based ZnO precursor material and (b) ZnO nanopowder prepared by heating the aloe-vera precursor material at 500 °C for 2h.

= L, e = microstrain of the sample; dimensionless, 2θ (degree) = diffraction angle; dimensionless, λ (nm) = wavelength; dimension = L]. The calculated D values by both the methods are nearly same. The present XRD study matches well with the XRD study of Barron et al, with hexagonal phases of ZnO [21]. A broad peak is obtained in the UV-vis spectra of ZnO at around 301 nm. The band gap calculated from the UV-vis spectra of ZnO is 3.35 eV.

Figure 2a shows the FTIR spectra of the aloe-vera based ZnO precursor sample before calcining at 500 °C. From the FTIR spectra, as seen in Figure 2a, a series of absorption peaks

Table 1

XRD data of ZnO nanopowders processed by heating the Aloe-vera based ZnO precursor in air at 500°C for 2h

d (nm)	I(%)	h k l
0.2815	55	(100)
0.2597	48	(002)
0.2478	100	(101)
0.1915	27	(102)
0.1624	47	(110)
0.1478	47	(103)
0.1406	15	(200)
0.1378	44	(112)
0.1363	23	(201)
0.1305	9	(004)
0.1237	10	(202)

from 500 to 4000 cm^{-1} are found, corresponding to the carboxylate and hydroxyl impurities in materials. A broad band at around 3465 cm^{-1} is assigned to the OH stretching mode of hydroxyl group. The peaks observed at 1638 and 1388 cm^{-1} are due to the asymmetrical and symmetrical stretching of the zinc carboxylate, respectively. On heating the aloe-vera based ZnO precursor material at 500 $^{\circ}\text{C}$ for 2h, the content of the carboxylate (COO^-) and hydroxyl ($-\text{OH}$) groups in the samples decreased, as seen in Figure 2b. The carboxylate probably comes from reactive carbon containing species during synthesis and the hydroxyl group results from the hygroscopic nature of ZnO [29]. These FTIR identified impurities in ZnO reduce significantly on heating the aloe-vera based precursor material at 500 $^{\circ}\text{C}$ for 2h. The spectral signatures of carboxylate impurities essentially disappear, indicating the possible dissociation of zinc carboxylate and conversion to ZnO during heating. Figure 2b shows a strong absorption band at around 436 cm^{-1} which corresponds to the E2 mode of hexagonal ZnO (Raman active) [29]. The band at around 500 cm^{-1} , as observed in Figure 2a, may be associated with oxygen deficiency and/or oxygen vacancy defect in ZnO [29], which reduces significantly (Figure 2b) on heating the polymeric precursor of ZnO at 500 $^{\circ}\text{C}$ for 2h.

Figure 3a shows the SEM micrograph of ZnO nanopowder prepared by heating the aloe-vera based ZnO precursor material at 500 $^{\circ}\text{C}$ for 2h in air. A very clean surface is seen by the SEM micrograph with the distinct particles. Particles are nearly spherical with hexagonal flakes and the particles are very uniformly distributed with an average particle size of 30-35 nm. EDX analysis provides the average composition throughout the sample (Fig. 3b).

The photodegradation of MeB was followed by measuring the absorbance of treatment samples. The absorbance of MeB was decreased with increasing time in the presence of ZnO and sunlight as shown in the Figure 4 and Table 2. The degradation percentage for MeB with a concentration of 7.815×10^{-6} M MeB was increased with time of illumination according to the following equation: $\text{Deg}\% = \{(A_0 - A_t) / (A_0 - A_a)\} \times 100\%$, A_t is the absorbance after time t and A_0 is the absorbance of dye at $t = 0$ time and A_a is absorbance at $t = 4$ hr. In fact, the photocatalytic activity of ZnO should be considered removing the contribution of natural degradation. But the natural degradation of MeB in sunlight has been measured to be very less in absence of ZnO catalyst. Only 5.8 % degradation of MeB in sunlight has been determined in 4h in absence of ZnO catalyst in the present investigation. This result matched well with the reported work [30].

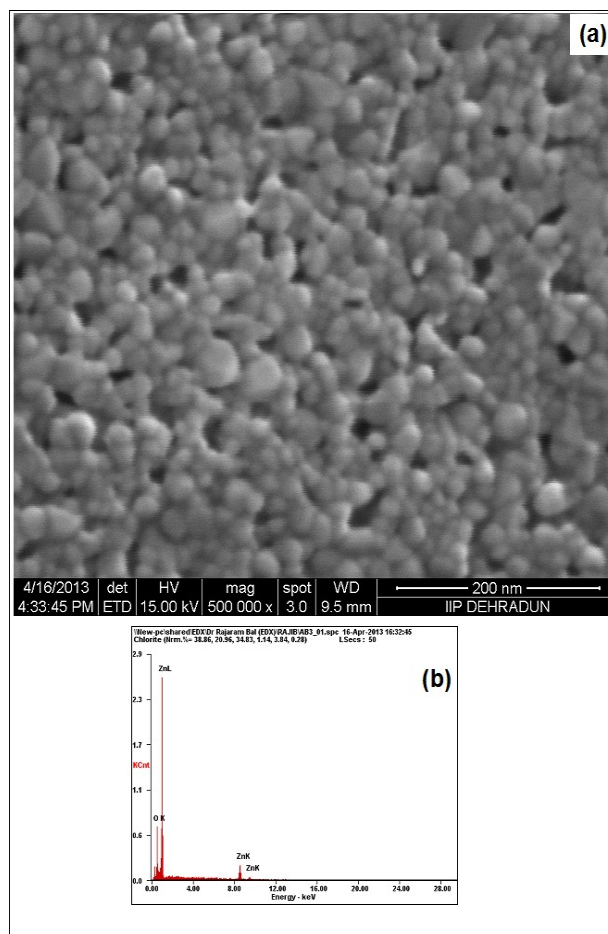


Fig. 3 - The (a) SEM micrograph and (b) EDX spectra of ZnO nanopowders prepared by heating the aloe-vera based ZnO precursor at 500 $^{\circ}\text{C}$ for 2h.

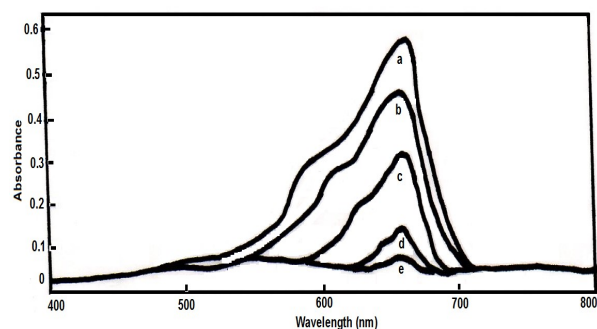


Fig. 4 - UV-Vis spectra of methylene blue treated with the photocatalytic reaction in presence of as prepared ZnO nanopowder at (a) starting of the reaction and after keeping (b) 1h, (c) 2h, (d) 3h and (e) 4h in sunlight.

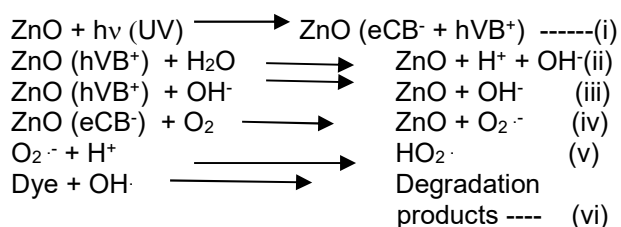
During the photocatalytic degradation of MeB, the conduction band electrons (e^-) and valence band holes (h^+) are generated when aqueous ZnO suspension irradiated with light energy greater than its band gap energy ($E_g = 3.2$ eV). The photo generated electrons could reduce the dye or react with electron acceptors such as

Table 2

UV-Vis spectra data of methylene blue treated with the photodegradation reaction in presence and absence of ZnO

Reaction condition	Peak (nm)	Absorbance (with ZnO)	Absorbance (without ZnO)
Starting solution	663.73	0.5493	0.5493
	613.35	0.3276	0.3276
After 1h kept in sunlight	663.73	0.4315	0.5448
	613.35	0.2306	0.3253
After 2h kept in sunlight	663.73	0.3053	0.5387
	613.35	0.1902	0.3215
After 3h kept in sunlight	663.73	0.1207	0.5278
	613.35	0.0914	0.3151
After 4h kept in sunlight	663.73	0.0740	0.5172
	613.35	0.0669	0.3087

O₂ absorbed on the Zn (II) surfacenor dissolved in water reducing it to super oxide radical anion O₂⁻. The holes generated by photochemical reactions can oxidize the organic molecule to form R[·] or react with OH⁻ or H₂O oxidizing them into OH[·] radicals. Together with other highly oxidant species (peroxide radicals) they are reported to be responsible for the heterogeneous ZnO photodecomposition of organic substrates as dyes. The photochemical reactions at the semiconductor surface which results the degradation of dyes can be demonstrated as follows:



The resulting OH[·] radical, being a very strong oxidizing agent (standard redox potential + 2.8 V) can oxidize most of MeB dye, the mineral end-products substrates not reactive toward hydroxyl radicals, are degraded employing ZnO photo catalysis with rates of decay, and highly influenced by the semiconductor valence band edge position [31].

4. Conclusion

Green synthesis method has been exploited for the preparation of ZnO nanoparticles with a p6₃mmc hexagonal crystal structure, by heating the precursor material at 500°C for 2h. The advantage of this method is that as prepared aloe-vera based ZnO precursor decomposes with combustion at a temperature of 500°C, resulting in crystallized ZnO nanopowders. Average crystallite size as measured from XRD is 30 nm and the band gap calculated from the UV-vis spectra of ZnO is 3.35

eV. The as prepared ZnO nanomaterials have been utilized for the photocatalytic degradation of methylene blue in aqueous medium. The photocatalytic degradation of methylene blue in ZnO suspension was carried out using solar irradiation. Colour change from blue to colorless was irreversible during the photodegradation process. The prepared ZnO nanomaterial has also a wide scope for the applications in solar cells, gas sensors, laser diodes, light emitting diodes, piezoelectric transducers, and in piezoelectric generators.

Acknowledgements

The authors would like to acknowledge Mr. Abhas Gaur for his help during the photodegradation experiments and in the UV-vis study.

REFERENCES

1. T.H. Yang, L.D. Huang, Y.W. Harn, C.C. Lin, J.K. Chang, C.I. Wu, J.M. Wu, High density unaggregated Au nanoparticles on ZnO nanorod arrays function as efficient and recyclable photocatalysts for environmental purification, *Small*, 2013, **9**, 3169.
2. Z. Liu, H. Bai, D.D. Sun, Hierarchical CuO/ZnO membranes for environmental applications under the irradiation of visible light, *Intern J Photoenergy*, 2012 Article ID 804840, 11 pages.
3. M.R. Nabid, R. Sedghi, S. Gholami, H.A. Oskooie, M.M. Heravi. Preparation of new magnetic nanocatalysts based on TiO₂ and ZnO and their application in improved photocatalytic degradation of dye pollutant under visible light, *Photochem and Photobio* 2013, **89**, 24.
4. L. Zhang, J. Yan, M. Zhou, Y. Yang, Y.N. Liu, Fabrication and photocatalytic properties of spheres-in-spheres ZnO/ZnAl₂O₄ composite hollow microspheres, *Appl Surf Sci*, 2013, **268**, 237.
5. L. Sun, D. Zhao, Z. Song, C. Shan, Z. Zhang, B. Li, D. Shen, Gold nanoparticles modified ZnO nanorods with improved photocatalytic activity, *J. Colloid Interface Sci* 2011, **363**, 175.
6. X. Bai, L. Wang, R. Zong, Y. Lv, Y. Sun, Y. Zhu, Performance enhancement of ZnO photocatalyst via synergic effect of surface oxygen defect and graphene hybridisation, *Langmuir*, 2013, **29**, 3097.
7. Y.L. Zhang, J.X. Zhao, Z.H. Ge, X.K. Zhao, L. Zou. ZnO/carbon quantum dots heterostructure with enhanced photocatalytic properties, *Appl Surf Sci*, 2013, **279**, 367.

8. B. Hu, J. Zhou, X.M. Wu, Decoloring methyl orange under sunlight by a photocatalytic membrane reactor based on ZnO nanoparticles and polypropylene macroporous membrane, *Intern J Polymer Sci*, 2013, Article ID 451398, 8 pages.
9. Khayyat, A. Suzan, M. Abaker, A. Umar, M.O. Alkattan, N.D. Alharbi, S. Baskoutas, Synthesis and characterizations of Cd-Doped ZnO multipods for environmental remediation application, *J Nanosci Nanotech*, 2012, **12**, 8453.
10. T. Xu, L. Zhang, H. Cheng, Y. Zhu, Significantly enhanced photocatalytic performance of ZnO via graphene hybridization and the mechanism study, *Applied Catalysis B: Environmental*, 2011, **101**, 4382.
11. Q. Wang, B. Geng, S. Wang, ZnO/Au hybrid nanoarchitectures: wet-chemical synthesis and structurally enhanced photocatalytic performance, *Environ Sci Technol*, 2009, **43**, 8968.
12. B. Liu, Z. Wang, Y. Dong, Y. Zhu, Y. Gong, S. Ran, Z. Liu, J. Xu, Z. Xie, D. Chen, G. Shen, ZnO-nanoparticle-assembled cloth for flexible photodetectors and recyclable photocatalysts, *J Mater Chem*, 2012, **22**, 9379.
13. A. Umar, M.S. Akhtar, A. Al-Hajry, M.S. Al-Assiri, N.Y. Almhbad, Hydrothermally grown ZnO nanoflowers for environmental remediation and clean energy applications, *Mater Res Bulletin*, 2012, **47**, 2407.
14. P.S.K. Sathish, A. Manivel, S. Anandan, Synthesis of Ag-ZnO nanoparticles for enhanced photocatalytic degradation of acid red 88 in aqueous environment, *Water Sci Technol*, 2009, **59**, 1423.
15. S. Chakrabarti, B. Chaudhuri, S. Bhattacharjee, P Das, B.K. Dutta, Degradation mechanism and kinetic model for photocatalytic oxidation of PVC-ZnO composite film in presence of a sensitizing dye and UV radiation, *J Hazardous Mater*, 2008, **154**, 230.
16. S.S. Shinde, P.S. Shinde, C.H. Bhosale, K.Y. Rajpure, Zinc oxide mediated heterogeneous photocatalytic degradation of organic species under solar radiation, *J Photochem Photobiol B: Biology*, 2011, **104**, 425.
17. P. Bansal, D. Sud, Photodegradation of commercial dye, Cl Reactive Blue 160 using ZnO nanopowder: Degradation pathway and identification of intermediates by GC/MS, *Separation and Purification Technol*, 2012, **85**, 112.
18. A. Bansal, R.J. Tayade, Effect of Dopants on ZnO Mediated Photocatalysis of Dye Bearing Wastewater: A Review, *Mater Sci Forum*, 2013, **757**, 165.
19. V. Etacheri, R. Roshan, V. Kumar, Mg-Doped ZnO nanoparticles for efficient sunlight-driven photocatalysis, *ACS Appl Mater Interfaces*, 2012, **4**, 2717.
20. L. Taccola, V. Raffa, C. Riggio, O. Vittorio, M.C. Iorio, R. Vanacore, A. Pietrabbissa, A. Cuschieri, Zinc oxide nanoparticles as selective killers of proliferating cells. *Intern J Nanomedicine*, 2011, **6**, 1129.
21. A. Thurber, D.G. Wingett, J.W. Rasmussen, J. Layne, L. Johnson, D.A. Tenne, J. Zhang, C.B. Hanna, A. Punnoose, Improving the selective cancer killing ability of ZnO nanoparticles using Fe doping, *Nanotoxicology*, 2012, **6**, 440.
22. N. Raghavan, T. Sakthivel, V. Gunasekaran, Enhanced photocatalytic degradation of methylene blue by reduced graphene-oxide/titanium dioxide/zinc oxide ternary nanocomposites, *Mater Sci Semiconductor Processing*, 2015, **30**, 321.
23. J. Xue, S. Ma, Y. Zhou, Z. Zhang, P. Jiang, Synthesis of Ag/ZnO/C plasmonic photocatalyst with enhanced adsorption capacity and photocatalytic activity to antibiotics, *RSC Adv*, 2015, **5**, 18832.
24. J. Xue, S. Ma, Y. Zhou, Z. Zhang, Facile synthesis of ZnO-C nanocomposites with enhanced photocatalytic activity, *New J Chem*, 2015, **39**, 1852.
25. J. Wang, Y. li, J. Ge, B.P. Zhang, W. Wan, Improving Photocatalytic Performance of ZnO via Synergistic Effects of Ag Nanoparticles and Graphene Quantum Dots, *Phys Chem Chem Phys*, 2015, **28**, 18645.
26. A.B. Lavand, Y.S. Malghe, Synthesis, characterization and visible light photocatalytic activity of nanosized carbon doped zinc oxide, *Intern J Photochem*, 2015, Article ID 790153, 9 pages.
27. S. Ram, T.K. Mandal, Synthesis and characterization of thin ferroelectric $\text{PbZr}_{0.52}\text{Ti}_{0.48}\text{O}_3$ fibrils, *J Amer Ceram Soc*, 2005, **88**, 3444.
28. T.K. Mandal, Characterization of tetragonal BaTiO_3 nanopowders prepared with a new soft chemistry route, *Mater Lett*, 2007, **61**, 850.
29. G. Xiong, K.B. Ucer, R.T. Williams, U. Pal, J.G. Serrano, Photoluminescence and FTIR study of ZnO nanoparticles: the impurity and defect perspective, *PHYSICA STATUS SOLIDI (C)*, 0002, No. z, zzz-zzz (2003) / DOI 10.1002/pssc.200300000.
30. H. Hassena, Photocatalytic degradation of methylene blue by using $\text{Al}_2\text{O}_3/\text{Fe}_2\text{O}_3$ nano composite under visible light, *Mod Chem Appl*, 2016, **4**, 000176.
31. M..R. Hoffman, S.T. Martin, W. Choi, D.W. Bahnemann, Environmental application of semiconductor photocatalysis, *Chem. Rev*, 1995, **95**, 69.
